

Analysis of Ca II 8542 scanning spectroscopy for statistical feature recognition

O. Malanushenko¹, H. Jones², M. Turmon³, and J. Pap⁴

¹ New Mexico State University, Department of Astronomy, Las Cruces, New Mexico, USA, e-mail: malanushenko@nmsu.edu

² National Solar Observatory, Tucson, Arizona, USA

³ JPL/Caltech, Pasadena, California, USA

⁴ University of Maryland College Park c/o NASA Goddard Space Flight Center Code 671.0, Greenbelt, MD, USA

Abstract. Previously, we used Bayesian methods to recognize active regions (AR), enhanced magnetic network (EN), and sunspots (SS) in National Solar Observatory/Kitt Peak Vacuum Telescope synoptic observations. In this paper we study imaging spectroscopy of the chromospheric Ca II 8542 Å and photospheric Fe I 8688 Å lines to improve separation of ARs and EN. We find that correlation plots between Ca line-center and ± 0.45 Å line-wing intensities show two identifiable but overlapping distributions. The first includes ARs (bright and faint) and the second includes ENs, network, and moat (“quiet Sun”). Active and Quiet distributions overlap in areas of EN and faint AR, so that feature identification using thresholds is unreliable. The statistical methodology of our previous work, however, is particularly well suited for distinguishing features with such partially overlapping distributions. Additionally, we find features in the Ca line which are not visible in the Fe observations, including a dark moat around an AR and narrow dark points associated with network and strong line-of-sight flows.

Key words. Sun: activity – Sun: sunspots – Techniques: spectroscopic – Techniques: image processing – Methods: data analysis

1. Introduction

In a previous study (Turmon et al. 2009) we applied Bayesian methods to identify active regions (AR), enhanced magnetic network (EN), and sunspots (SS) in National Solar Observatory/Kitt Peak Vacuum Telescope (KPVT) Fe I 8688 Å synoptic observations (Jones et al. 1992) from 1992 to 2003. Using images of magnetic field, continuum intensity, and equivalent width, we found that we could

distinguish the three kinds of regions but that the AR and EN classes were significantly intermixed. In this research we study KPVT scanning spectroscopy of selected areas in both the chromospheric Ca II 8542 Å and photospheric Fe I 8688 Å lines to analyze spectra in different features and try to find differences between network and active regions for recognition purposes. The success of such a feature recognition application strongly depends on the separability of observable parameters characterizing the different features.

Send offprint requests to: O. Malanushenko

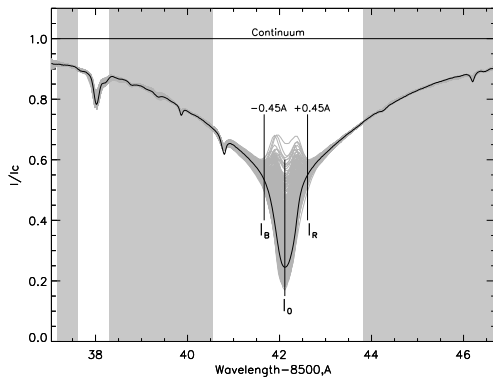


Fig. 1. Subset of reduced Ca spectra observed on 2001 May 4, with over-plotted NSO solar atlas spectrum (bold). Shaded spectral zones are used for continuum determinations. Marked wavelengths are used to form images for data analysis.

2. Observations and data reduction

Six sets of observations were taken on 2000 May 4–6 in the Ca and Fe lines using the NASA/NSO Spectromagnetograph (SPM) at the KPVT. A CCD camera recorded spectra along the entrance slit and a scanning system stepped the solar image perpendicular to the slit to produce an image. Dark and flat corrections were applied using a special technique developed for synoptic observations at the KPVT (Jones 2003). The spectral dispersion of the observations was $0.045 \text{ \AA pix}^{-1}$ and the spectral range was 10 \AA . The wavelength scale was determined by matching the average wavelength positions of nearby solar lines to those in the NSO atlas (Wallace et al. 1993). The spatial scale was $1''10 \text{ pix}^{-1}$, and we determined spatial coordinates by comparing our observations to sunspot and plage contours derived from synoptic KPVT images.

Within the Fe spectral range, we were able to determine a continuum level from a polynomial fit to the intensity at wavelengths free from spectral lines. However, the Ca line is wider than the SPM spectral range, and no continuum is included in the observations. To determine the nearby continuum we adapted a spectral standard technique developed for He I 1083 nm spectral observations (Malanushenko, & Jones 2004). Using

this method we forced spectra to be the same as the Atlas spectrum in those spectral zones in the Ca wings where the changes originated mostly from continuum variations. This is a reasonable assumption as the solar variability occurs almost entirely in the core region of the line. It is varying from a pure absorption profile to a self-reversed emission core similar to the Ca II H and K lines, the upper levels of which are shared with the infrared triplet including the 8542 Å line. Images in spectral zones away from the core are similar to KPVT continuum images. Figure 1 shows a subset of the Ca line profiles.

3. Data analysis

For our analysis we used KPVT magnetic flux (MF) and continuum images from synoptic observations: Ca images at line center (I_0) and $\pm 0.45 \text{ \AA}$ into the line wings (I_R and I_B); and Fe images in line center and at $\pm 0.13 \text{ \AA}$ into the wings. The wavelengths of the selected Ca images are marked in Fig. 1. One set of observations is presented in Fig. 2. The area of observations included NOAA 9445 and its nearby magnetic network. We identified different features in the images using contours and the network pattern. We used the KPVT continuum image for SS identification; the Ca I_0 image for AR, network and cells, and dark moat; I_B for the bright part of AR and dark points around the network. A list of selected features and the parameters for their identification is summarized in Table 1.

The Ca I_0 map shows the AR surrounded by a dark “moat” and a pattern of network and its cells. Contour #1 outlines the AR and enhanced network. The same contour in the MF image shows a good correspondence between the magnetic network and enhanced network in I_0 . This same contour, over-plotted with the Fe line center image, emphasizes low contrast plage. Contour #2 shows the dark moat around the AR, which probably corresponds to a “circumfacula” described by Harvey (2005). Enhanced and weak network as well as cell centers are visually apparent in Ca I_0 but their intensity is intermixed and we cannot use contours or thresholds to distinguish properly be-

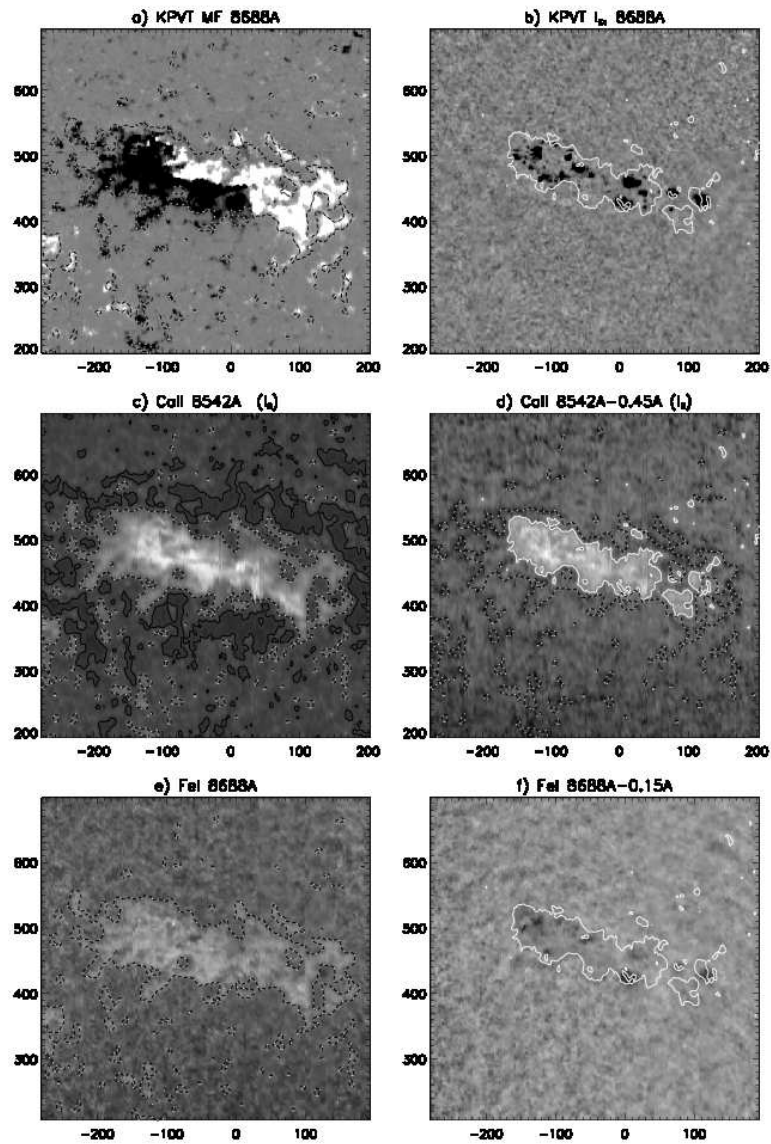


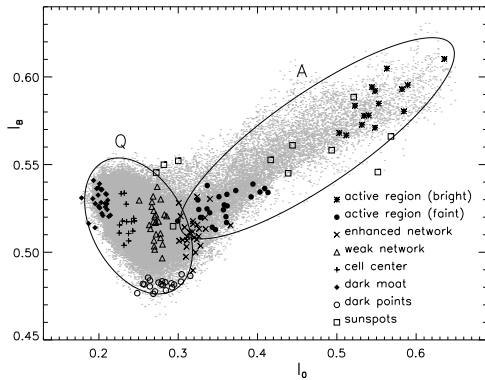
Fig. 2. Observations for 2001 May 04. The images are: KPVT MF (a) and continuum (b); Ca line center I_0 (c) and blue wing I_B (d); Fe line center (e) and Fe line wing (f). Dashed white-black contour (#1) is $I_0 = 0.29$ which separates AR and EN from quiet areas. Black contour (#2) is a dark moat around AR with $I_0 = 0.22$. The white solid contour (#3) separates the bright core of the AR with $I_B = 0.55$. These three contours are over-plotted with other images for discussions.

tween them. The AR is bright (contour #3) in I_B but has smaller area than in I_0 or MF. Contour #3 on the KPVT continuum image

entirely contains all sunspots which appear in the core of the AR. The network contrast is less in the Ca line wings, disappearing entirely

Table 1. List of areas and spectral parameters.

Feature	Identification	FWHM	R_0	V_{LOS} [km s ⁻¹]
sunspots	$I_c < 0.92$	1.00	0.59	0.35
AR bright	$I_B > 0.55$	1.84	0.45	0.17
AR faint	$I_B < 0.55$ and $I_0 > 0.29$	0.85	0.65	-0.21
enhanced network	$I_0 > 0.29$, detached from AR	0.84	0.67	-0.26
weak network	$I_0 \approx 0.27$, visual selection	0.71	0.73	-0.12
cell centers	$I_0 \approx 0.23$, visual selection	0.63	0.77	-0.28
dark points, blue	$I_B < 0.50$	0.80	0.73	-0.98
dark points, red	$I_R < 0.50$	0.83	0.73	1.19
dark moat	$I_0 < 0.22$	0.54	0.81	-0.09

**Fig. 3.** Correlation plot for Ca I_B vs I_0 . Grey area represents subset of all pixels in our images. The values for selected features are over-plotted with different symbols. Two overlapped distributions on the plot are labeled as “A” and “Q”.

at ± 0.45 Å from line center although small, isolated, dark points can be found attached to some network areas. Patterns of dark points are not similar in I_R and I_B maps which prompts additional analysis. SSS are visible in Fe continuum, Ca continuum, and Fe line-wing (even normalized to the continuum) images.

We selected 10–15 representative spectra of the features and calculated the line depth R_0 , the FWHM, and the line-of-sight velocity V_{LOS} for their average spectra (see Table 1). R_0 was calculated using a continuum level of 1.0, but a quasi-continuum level at $0.72 I_c$ was used for the calculation of FWHM. Parameters of faint ARs and enhanced network are very similar. The dark moat is the darkest area in Ca I_0 and the line is also at its narrowest there.

Dark points are similarly identified on I_R and I_B , and have measurable line-of-sight flows of about 1 km sec^{-1} .

A correlation plot between intensity Ca I_B vs I_0 is presented on Fig. 3. There are two kinds of distributions on the plot. The first, A, represents the bright and faint ARs, and the second, Q, combines all other quiet Sun features. They partially overlap at faint AR (A) and EN (Q) areas. SSS are spread out through the whole plot and may not be classified in this way.

4. Conclusions

We analyzed SPM scanning spectroscopy in the Ca II 8542 Å line to emphasize differences between AR and EN. The correlation plot of Ca images in line center and -0.45 Å line-wing intensities shows two distributions with different properties. The first includes ARs (bright and faint), and the second contains less active “quiet”-Sun features (ENs, network, moat). AR and Quiet distributions overlap in areas of EN and faint AR. Features with observed or derived quantities in the overlapping regions of these distributions cannot be reliably distinguished using thresholds, but their separation should be amenable to our statistical analysis. We also found additional phenomena which include the dark moat around ARs and the small Ca line dark points associated with network with strong line-of-sight flows of up to 1 km sec^{-1} . To verify these results we plan to repeat this analysis using SOLIS observations. This research may be important for automatic monitoring of solar activity.

Acknowledgements. This work is supported by NASA/Solar and Heliospheric Physics grant SHP04-0037-0099. KPVT data used here were provided cooperatively by AURA/NSO, NASA/GSFC, and NOAA/SEL. We thank Dr. V. Malanushenko for valuable consultations regarding the spectral analysis.

References

- Jones, H. P. 2003, Sol. Phys., 218, 1
- Jones, H. P. et al. 1992, Sol. Phys., 139, 211
- Harvey, J. W. 2005, AGU Spring Meeting, abstract #SP41B-05
- Malanushenko, O. V. & Jones, H. P. 2004, Sol. Phys., 222, 43
- Turmon, M., Jones, H. P., Malanushenko, O. V., & Pap, J. M. 2009, Sol. Phys., accepted
- Wallace, L., Hinkle, K., & Livingston, W. 1993, NSO Technical Report #93-001